

500 kA Cell Coke Preheating Optimization

Yongquan Huang¹

1. Support Engineer

Guangxi Hualei New Materials, Baise, China

Corresponding author: 541781533@qq.com

<https://doi.org/10.71659/icsoba2025-al015>

Abstract

Electrical preheating using coke bed [1, 2] is the primary preheating method to start aluminium reduction cells. Preheating quality significantly impacts the start-up, normalization and future operation of the cells. During this study, coke grain sizes, coke bed preparation and the installation of anode flexible connections before the start-up of a 500 kA cells were optimized to increase the uniformity of anode current distribution during preheating. Simultaneously, the cell preparation method was improved by covering the anode surface to reduce material drop on the cell cathode and sealing the central channel between anodes to increase cavity tightness. This ensures that the high-temperature flue gas generated during preheating stays longer inside the cell cavity. Additionally, the optimized method of removing shunting plates extends the current shunting time. These measures collectively promote uniform heating throughout the cell cavity, reduce the cell voltage during preheating and lower energy consumption.

Keywords: 500 kA aluminium reduction cell, Coke preheating, Current shunting, Flue gas waste heat, Preheating voltage.

1. Introduction

Cell preheating quality directly impacts cell stability during start-up and early operation, thereby influencing the formation of the ledge during this phase. Poor preheating and start-up performances can lead to unstable operation during the normal operation, to significant variations in energy consumption and to increased workload to manage abnormal situations and even affect the cell life. The 500 kA potline at a smelter comprises 300 cells, all using electrical preheating before start-up. In recent years, the smelter has improved the uniformity of anode current distribution during preheating and increased preheating effectiveness. The coke/graphite ratio in the material used to prepare the bed on which the anode lies during preheating was optimized and the coke bed thickness reduced. However, some cells still exhibit issues like excessive noise, poor stability, and difficulty in voltage reduction after start-up, during early operation. These cells fail to operate stably during normal production. For instance, under identical current efficiency, cell A requires 40 mV higher set voltage than cell B, resulting in higher energy consumption. As the smelter has ambitious production and energy consumption targets, it is imperative to further optimize cell preheating to lay a solid foundation for stable cell operation.

2. Main Operational Steps of Cell Preheating

The main operational steps of cell preheating are cell preparation and energization.

2.1 Cell Preparation

When a cell is shut down and undergoes maintenance, a new lining is installed and inspected. Then cell preparation can start. First, dust on the cathode surface is blown away. Then the coke bed on which the anode will rest during preheating is installed on the cathode surface. The anodes are lowered on the coke bed using a multi-functional crane, ensuring their bottom surfaces make

full contact with the coke particles. Flexes are manually installed to link the aluminium anode stem with the anode beam. These steps are repeated until all 48 anodes are installed in the cell. Next, the anodes are covered with crushed bath, cryolite, and soda ash that are evenly spread over the top the anode surface.

2.2 Power-on

After preparation, six sets of shunting plates (two shunting plates per set) are mounted on the cell's downstream anode beam and connected to the six anode risers of the downstream cell. Then, using a non-power-cut cell start-up device on the cell upstream, the cell is energised. The non-power-cut cell start-up device is removed, completing the power-on process. At this stage, the cell has started its preheating. During this phase, the coke bed acts as a resistive heating element, simultaneously heating the anode and cathode carbon blocks [3]. After 96 hours of preheating, the anode and all the elements forming the cell cathode lining reach their target temperature, meeting the conditions for the next start-up phase.

3. Preheating Optimization

In response to issues such as excessive noise, significant voltage deviation, and poor stability observed in newly started cells during their early operation, repeated analysis and discussions were conducted. It was decided to optimize preheating using Cell X as the reference cell and Cell Y as the test cell.

3.1 Coke Bed Optimization

The coke used in this smelter to make the coke bed had a particle size range of 2–6 mm. The relatively large particle size resulted in incomplete contact between the anode carbon block bottom and the coke particles during anode setting, reducing the effective conductive area after power-on. Additionally, uneven particle size distribution affected the uniformity of anode current distribution during preheating, badly impacting anode thermal expansion and lining temperature distribution. To address this issue, the smelter adopted a pre-treatment method involving coke mechanical crushing to refine the particles. Simultaneously, new sieving screens were made to precisely maintain coke particles within a 2–4 mm range. Additionally, the smelter also produced specialized tools to improve the coke bed quality, aiming at maximizing the contact area between the coke particles and the anode carbon block. This increased the effective conductive area, achieving a more balanced anode current distribution and promoting uniform heating and expansion of the anode.

3.2 Preheat Flex Installation

After repeated use, the two contact surfaces of the flexes became uneven, preventing full contact with the anode stem and the cell anode beam, thereby reducing the conductive area. These contact surfaces were polished along with the anode stem and the anode beam, improving the contact voltage drops and the uniformity of anode current distribution after power-on.

3.3 Optimizing Anode Cover During Cell Preparation

Originally, the top of the central channel was not closed when preparing the cell. The high-temperature flue gas generated during preheating escaped directly through this channel, resulting in significant heat loss and insufficient preheating temperature. Additionally, the gaps between anode were not closed during covering, causing material to fall into these gaps. As a result, when the anode heated and expanded during preheating, it could expand upwards only rather than sideways, generating uneven anode current distribution during preheating. To address this issue,

the smelter developed slabs made of crushed bath. During cell preparation, before the first anode cover, the cell central channel had been covered with these slabs, and the gaps between anode carbon blocks were plugged with crushed bath. This increased the sealing of the central channel and prevented material from filling the anode gaps. The high-temperature flue gas generated during preheating was then circulating within the sealed cavity. This promoted more uniform current flow and thermal expansion of the anode carbon blocks, and ensured even heating of the cell lining. As a result, cell voltage during preheating was reduced. [3, 4].

3.4 Shunt Removal Optimization

As shown in Figure 1, the 500 kA the cells have six anode risers, numbered from top to bottom as the first to the sixth. Each anode riser is connected to 2 shunts, corresponding to shunts 1–12, also arranged from the top to the bottom of the picture. Each shunt connects the anode beam of the cell in preheating to an anode riser of the downstream cell.

The original shunt removal method involved detaching two plates from the same riser at a time, with each group of 2 shunts removed at one-hour intervals. However, simultaneously removing two shunts from the same riser leads to significant localized current distribution deviations, which may cause local cathode overheating and early cathode damage. The shunt removal sequence was then improved. One shunt was removed on two different anode risers every 8 hours. This approach reduced the impact of shunt removal on the anodes and cathodes in the corresponding areas, ensuring more uniform anode current distribution. Extended interval between shunt removals, prolonged the current shunting duration and reduced the energy consumption during preheating.

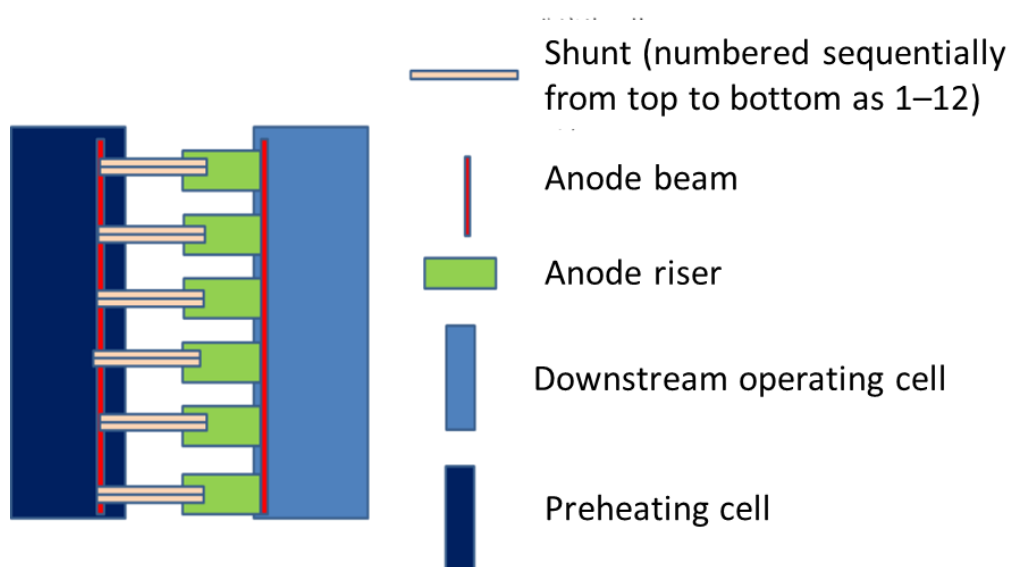


Figure 1. Schematic diagram of shunt connection during cell preheating.

4. Results and Discussion

To verify the effect of the optimization measures, statistical tracking was conducted on data including the anode current distribution after power-on, average voltage during the preheating period, anode uplift, as well as the average voltage and noise during early operation.

4.1 Anode Current Distribution

As shown in Figures 2–5, when the conventional preheating was used, the current was the lowest at A1 and A24 (0.2 mV) and the highest at A11 (3.1 mV). Note that the anode current was measured with a mV fork applied to each anode in sequence; anode current is proportional to the mV voltage drop between the two pins of the fork. Between A1 and A24, the current had significant fluctuations multiple times, with a maximum difference of 2.9 mV, indicating poor uniformity in the current distribution across the upstream anodes. In contrast, when the optimized preheating method was applied, the current flowing through the upstream anodes remained between 1 and 1.4 mV from A1 to A24, with a maximum difference of only 0.4 mV and only few fluctuations. The same was observed on the downstream side. The optimized preheating method significantly improved anode current distribution during preheating.

1.

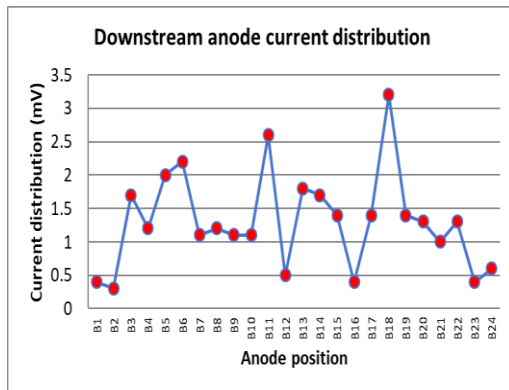


Figure 2. Upstream anode current distribution during conventional preheating (Cell X).

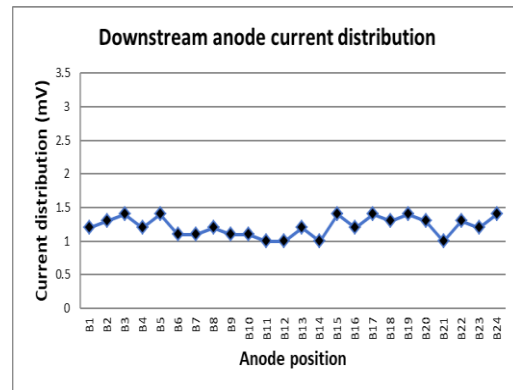


Figure 3. Upstream anode current distribution during optimized preheating (Cell Y).

2.

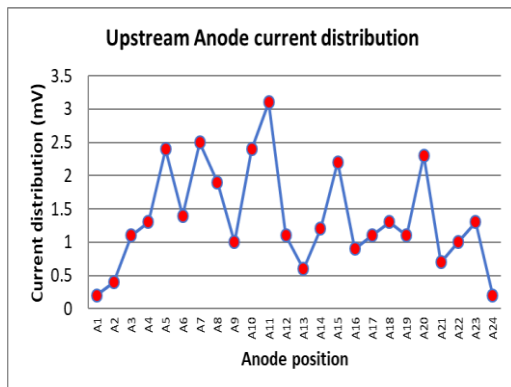


Figure 4. Downstream anode current distribution during conventional preheating (Cell X).

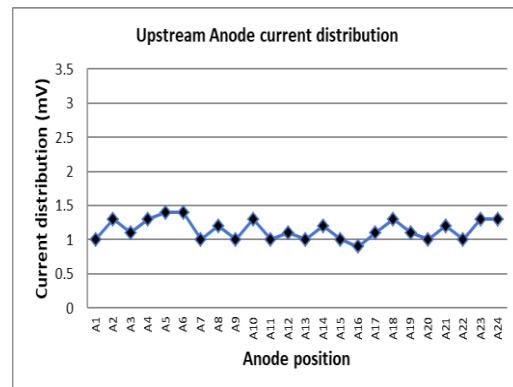


Figure 5. Downstream anode current distribution during optimized preheating (Cell Y).

4.2 Anode Uplift

According to Figures 6–9, during conventional preheating, the anode uplift of A24 is the smallest (1.4 cm), A14 was the maximum (9.6 cm). The anode uplift distribution between A1 and A24 is low at both ends and high in the middle, with maximum difference of 8.2 cm. The total uplift sum from A1 to A24 is 140.8 cm. With the optimized preheating, the upstream anode uplift is still low at both ends and high in the middle, but the maximum uplift reduces to 6.4 cm and the minimum increases to 2.5 cm, narrowing the difference to just 3.9 cm. The total uplift sum from A1 to A24

decreases to 116.8 cm, 24 cm lower than the conventional method. A similar trend was observed for the downstream anodes.

3.

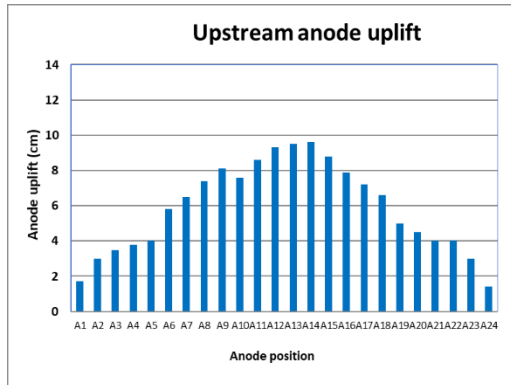


Figure 6. Upstream anode uplift with conventional preheating (Cell X).

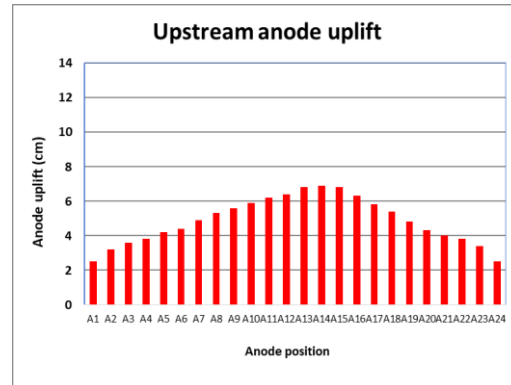


Figure 7. Upstream anode uplift with optimized preheating method (Cell Y).

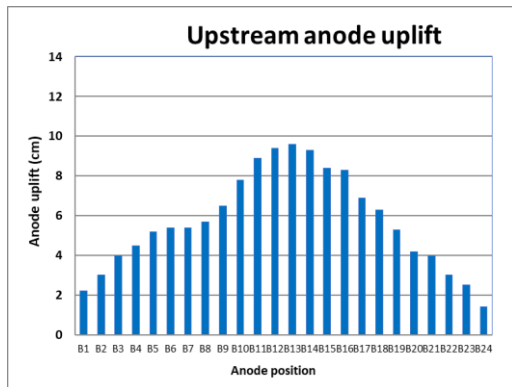


Figure 8. Downstream anode uplift with conventional preheating method (Cell X).

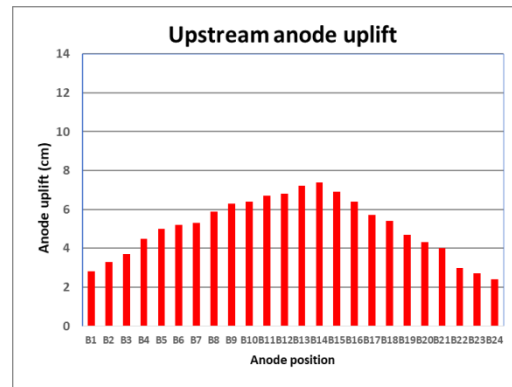


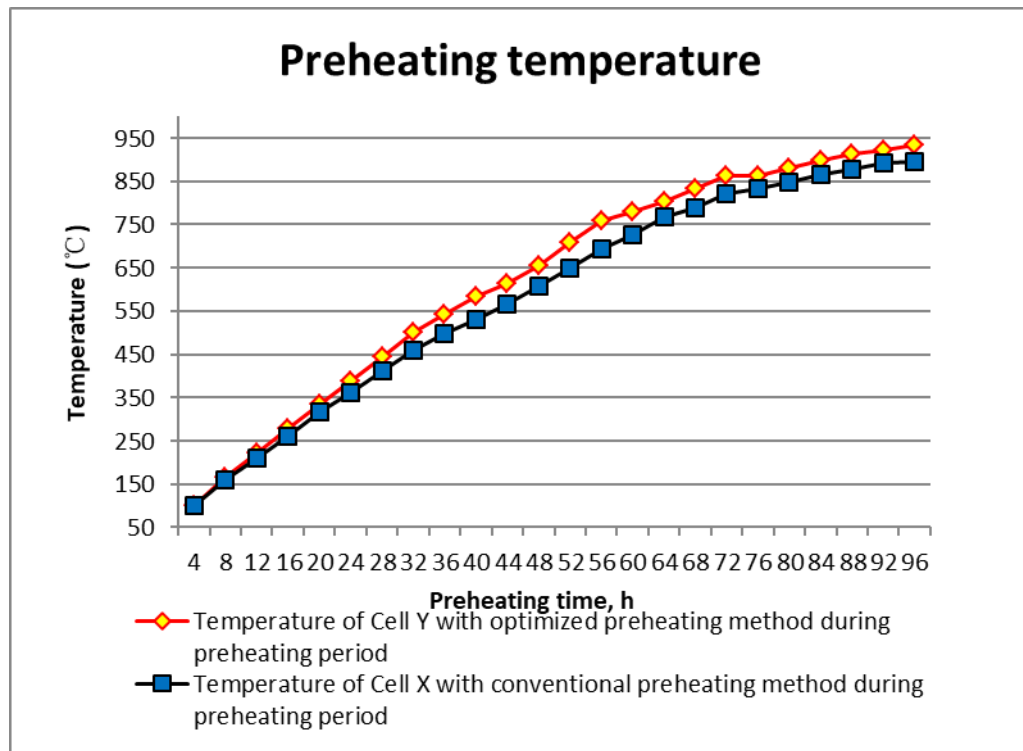
Figure 9. Downstream anode uplift with optimized preheating method (Cell Y).

4.3 Temperature and Voltage During Preheating

Figure 10 shows that in conventional preheating, the maximum preheating temperature of the cell reached only about 890 °C. In optimized preheating, the peak preheating temperature was approximately 930 °C. During the first 24 hours of preheating, the temperature curves of both methods were nearly identical, but thereafter, Cell Y (optimized preheating) had consistently higher temperatures than Cell X (conventional preheating).

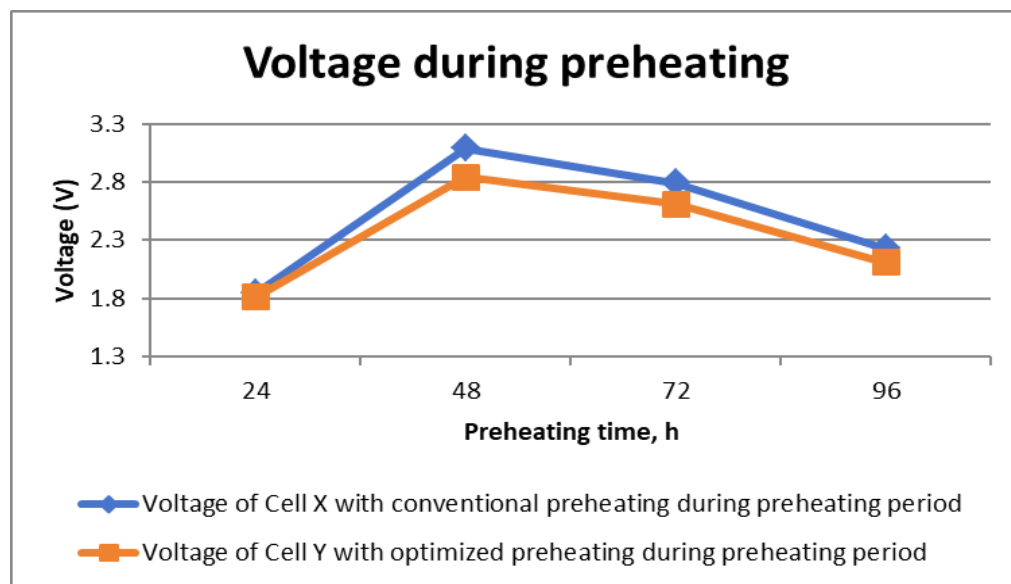
Figure 11 gives cell voltages during preheating. Cell X maintained higher voltages throughout the process than Cell Y, with an average voltage difference of 14 mV over the preheating period.

With the better sealing of the central channel using bath slabs, Cell Y had improved thermal insulation. During preheating, it had lower voltage while delivering higher preheating temperature.



4.

Figure 10. Conventional and optimized preheating temperature over time.



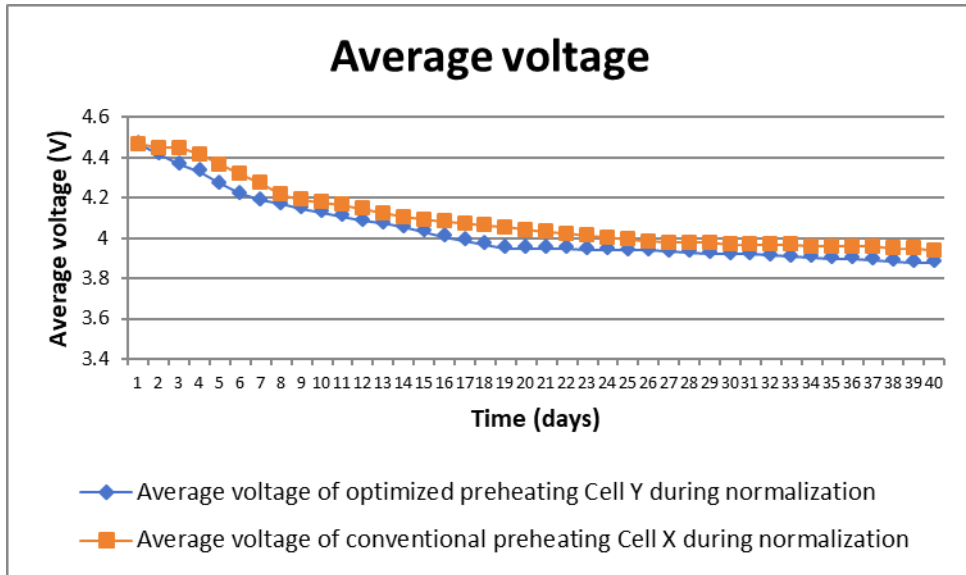
5.

Figure 11. Voltage variation during preheating in conventional vs. optimized preheating electrolytic cells.

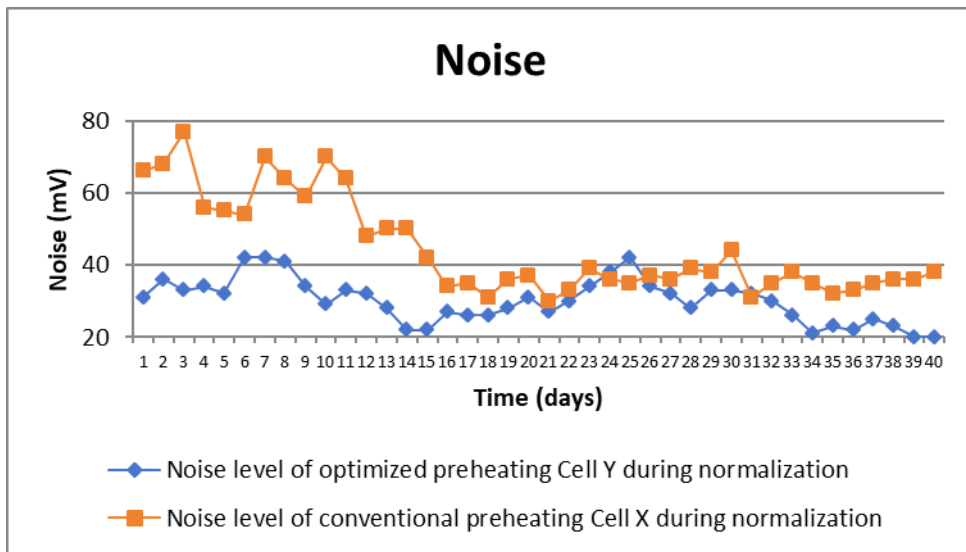
4.4 Voltage Deviation and Noise During Early Operation

Early operation last 40 days after cell bath-up. As shown in Figures 12–13, Cell X, had abnormally high noise in the first 15 days after start-up, with maximum noise reaching nearly 80 mV and an average noise of 45 mV. Even one month after start-up, its noise remained around 35 mV. In contrast, Cell Y showed significantly lower noise during the first 40 days of early operation, with maximum noise of only about 40 mV and the average noise of 30 mV. During the complete early operation period, the average voltage of Cell Y was consistently lower than that of Cell X, saving

an average of 63 mV per day. Cell Y had better stability and lower energy consumption than Cell X during early operation.



6. **Figure 12. Average cell voltage of conventional preheating vs. optimized preheating cells.**



7. **Figure 13. Noise comparison between conventional preheating cell and optimized preheating electrolytic cell.**

5. Conclusions

An optimized cell preheating method was developed and the results were compared to the conventional one. The optimized preheating allowed to reduce the cell voltage and the energy consumption during the preheating while increasing the maximum preheating temperature after 96 hours of preheat. During the 40 days of early operation, the average noise value of the optimized preheating cell was by 15 mV lower than the noise of the conventional preheating. The average voltage of the optimized preheating cell was by 63 mV lower than the conventional one. This is important for forming a high-quality ledge [5, 6] in newly started cells and lays solid foundation for efficient, low-energy and long-life operation of the cells.

6. References

1. Naixiang Feng, *Aluminium Electrolysis*, Beijing: Chemical Industry Press, 2006 (in Chinese).
2. Yexiang Liu, Jie Li, et al., Modern Aluminium Electrolysis, *Beijing: Metallurgical Industry Press*, 2008, 335–336 (in Chinese).
3. Yanhai Feng, Xinxi Wang, Simulation and Optimization of Thermal Field during Coke Particle Preheating Process in 300 kA Aluminium Reduction Cell, *Transactions of Nonferrous Metals Society of China*, 2007 (8), 1–5 (in Chinese).
4. Zhuxian Qiu, *Pre-baked Channeled Aluminium* (3rd Edition), Beijing: Metallurgical Industry Press, 2005 (in Chinese).
5. Yarui Gao, Lifu Han, Production Practice of Reducing Black Voltage in 306 kA Electrolytic Cells, *China High Technology Enterprises*, 2013 (19), 142–145 (in Chinese).
6. Guowei Li, et al., Preheating Start-up and Operation Practice of SY500 kA New Energy-saving Pot, *Light Metals*, Issue 7, (2020), 24–28 (in Chinese).